SUPPORTING INFORMATION

Oxidation of Iron Causes Removal of Phosphorus and Arsenic from Streamwater in Groundwater-Fed Lowland Catchments

STIJN BAKEN*, PETER SALAETS, NELE DESMET, PIET SEUNTJENS, ELIN VANLIERDE, ERIK SMOLDERS

CONTENTS

1. Description of the studied catchments

The location of the studied catchments is shown in Figure S 1. Two hydrogeological sections are shown in Figure S 2. The Central Campine groundwater system is separated from the Brulandkrijt groundwater system underneath it by the Boom clay aquitard. Therefore, in the studied part of the Kleine Nete and Demer catchments, the Central Campine groundwater system is the only phreatic groundwater body. Within the Central Campine system, the Diestiaan aquifer likely contributes most to stream flow, due to its thickness and high permeability[1]. The Diestiaan consists of glauconitic sands which supply large amounts of Fe(II) to the groundwater[2].

The water balances in the study area have been studied extensively by Batelaan (2006)[3], using the MODFLOW and WetSpass models. MODFLOW is a three dimensional groundwater model; WetSpass is a steady state spatially distributed water balance model for simulating average groundwater recharge, evapotranspiration, runoff, and interception [4]. The estimated year-averaged surface runoff, evapotranspiration, and groundwater recharge in the Nete and Demer catchments were estimated with WetSpass and MODFLOW (Figure S 3). Groundwater recharge exceeds surface runoff by factors 7 (Nete catchment) and 4 (Demer catchment). Because we studied the part of the Demer catchment with a relatively flat topography, the runoff in the studied part of the Demer catchment is likely lower than the estimates shown here. The average annual precipitation is 773 (Nete catchment) and 756 mm yr^{-1} (Demer catchment). Figure S 4 shows the modelled year-averaged groundwater discharge and recharge in the study area. Discharge mostly occurs along the streams, highlighting that the streams in the study areas mostly gain groundwater. Separation of the baseflow contribution from the total hydrograph (Figure S 5) shows that year-averaged baseflow contributions to stream flow in the study area range between 71 and 83%. Finally, Figure S 6 shows that there is an excellent correlation between modelled groundwater discharge and observed baseflow in streams.

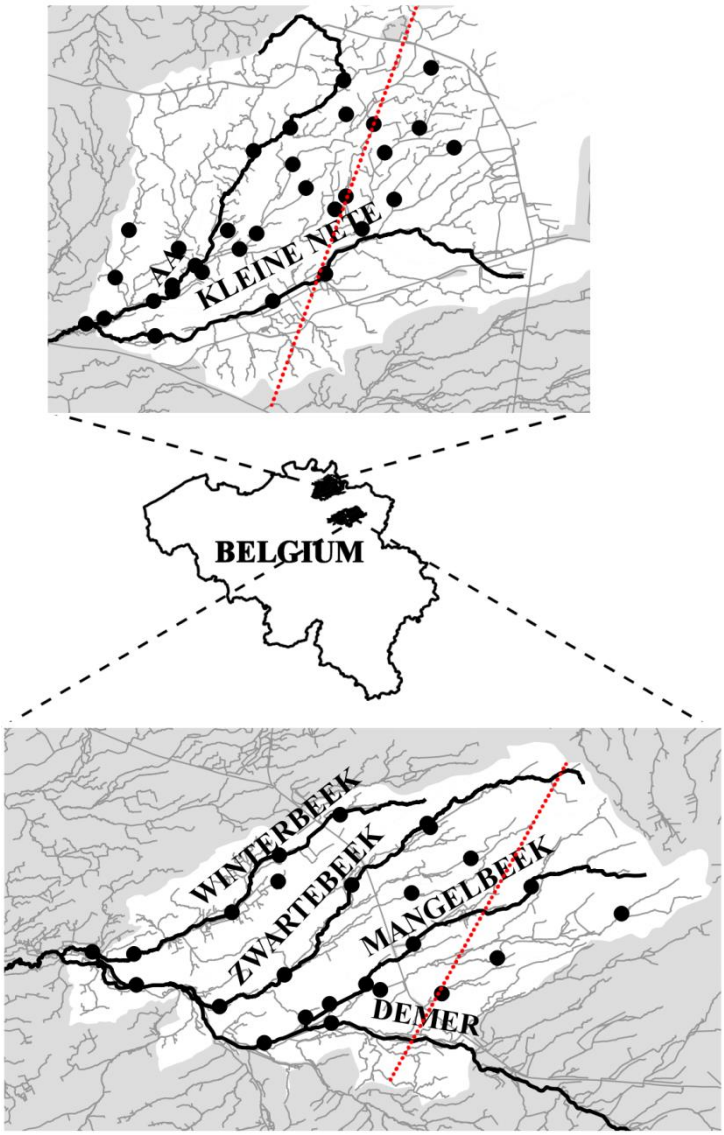

Figure S 1: Map of Belgium with the study areas indicated: the Kleine Nete catchment upstream of the town of Grobbendonk (top) and the three northern tributaries to the Demer river. The major streams (black lines), minor streams (gray lines), and the sampling locations (black dots) are indicated. The red dotted lines indicate the location of the hydrogeological cross sections (Figure S 2).

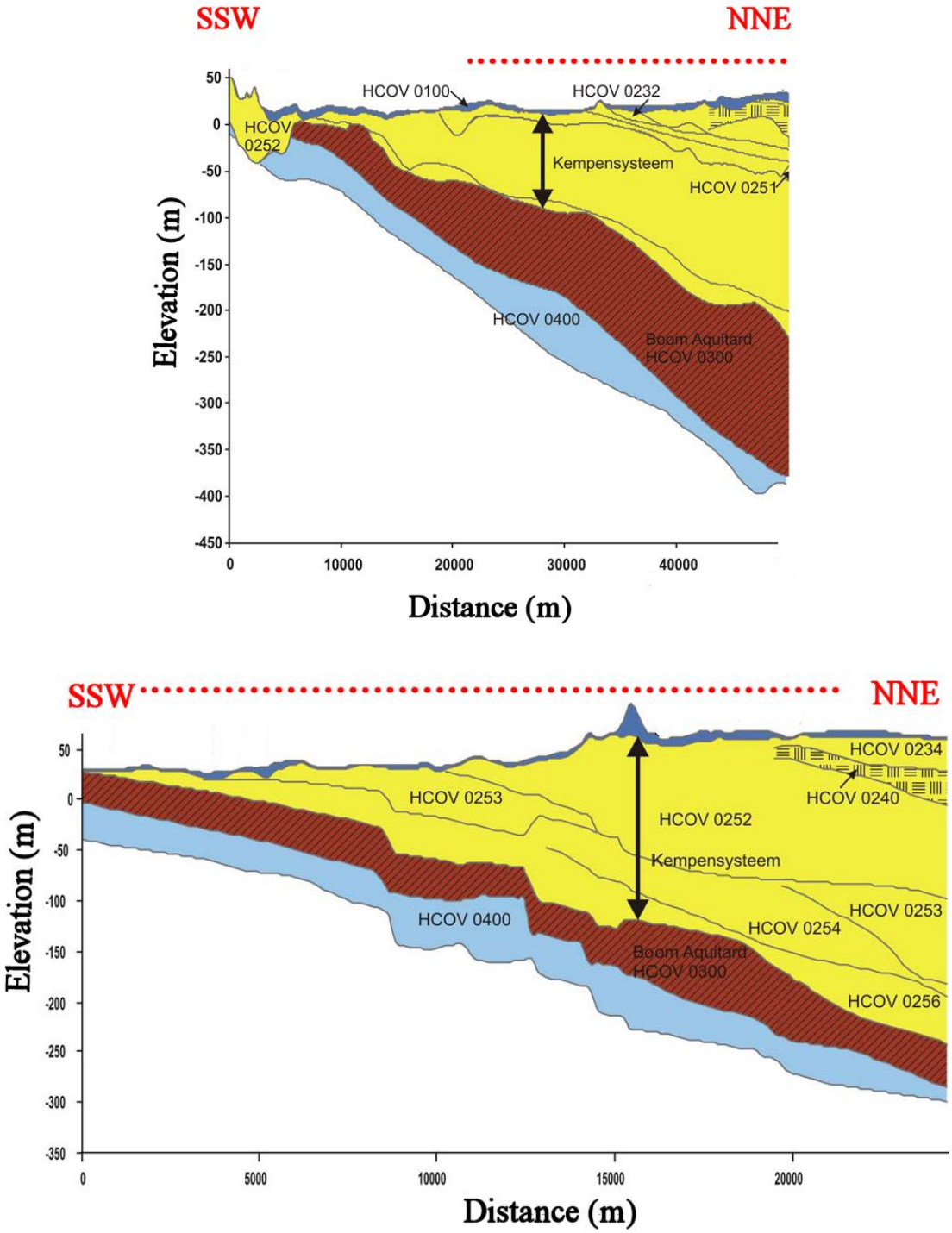

Figure S 2: Hydrogeological profile along SSW-NNE sections across the Kleine Nete catchment (top) and the northern part of the Demer catchment (bottom), adapted from ref.[5]. The dotted red lines indicate the location of each section as shown in Figure S 1. The Central Campine groundwater system (yellow) is the only phreatic groundwater body in the study area; it is separated from the Brulandkrijt groundwater system (blue; only top layer shown) by the Boom clay aquitard (brown).

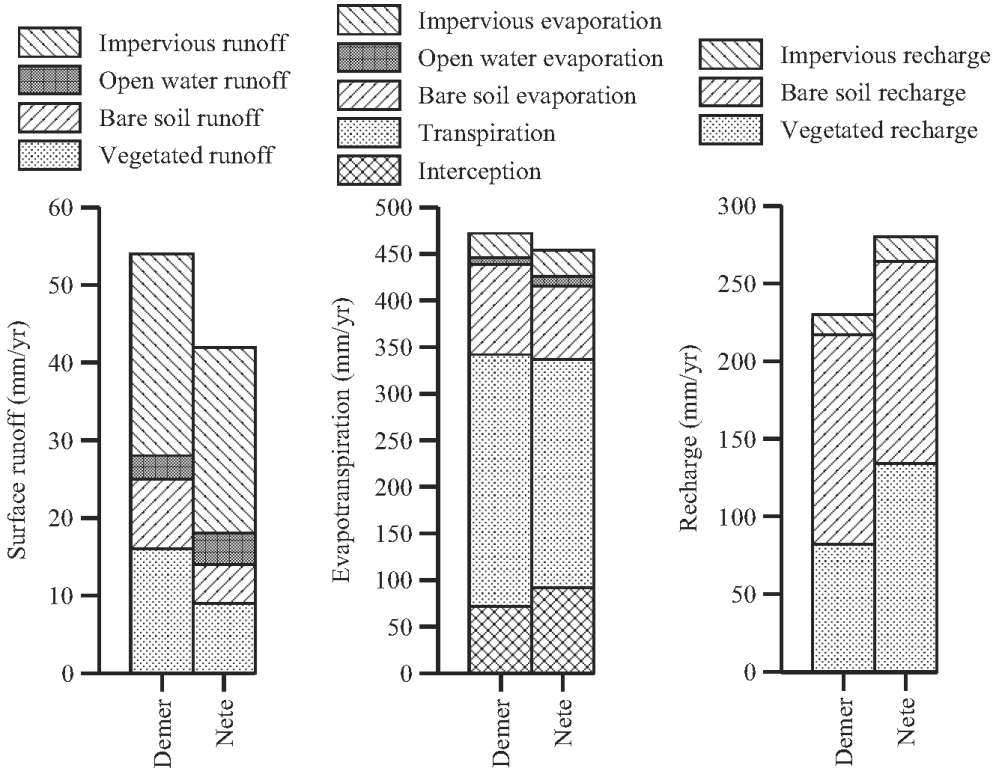

Figure S 3: Average annual surface runoff, evapotranspiration, and groundwater recharge in the Nete and Demer catchments, calculated using the WetSpass and MODFLOW models (adapted from ref.[3]).

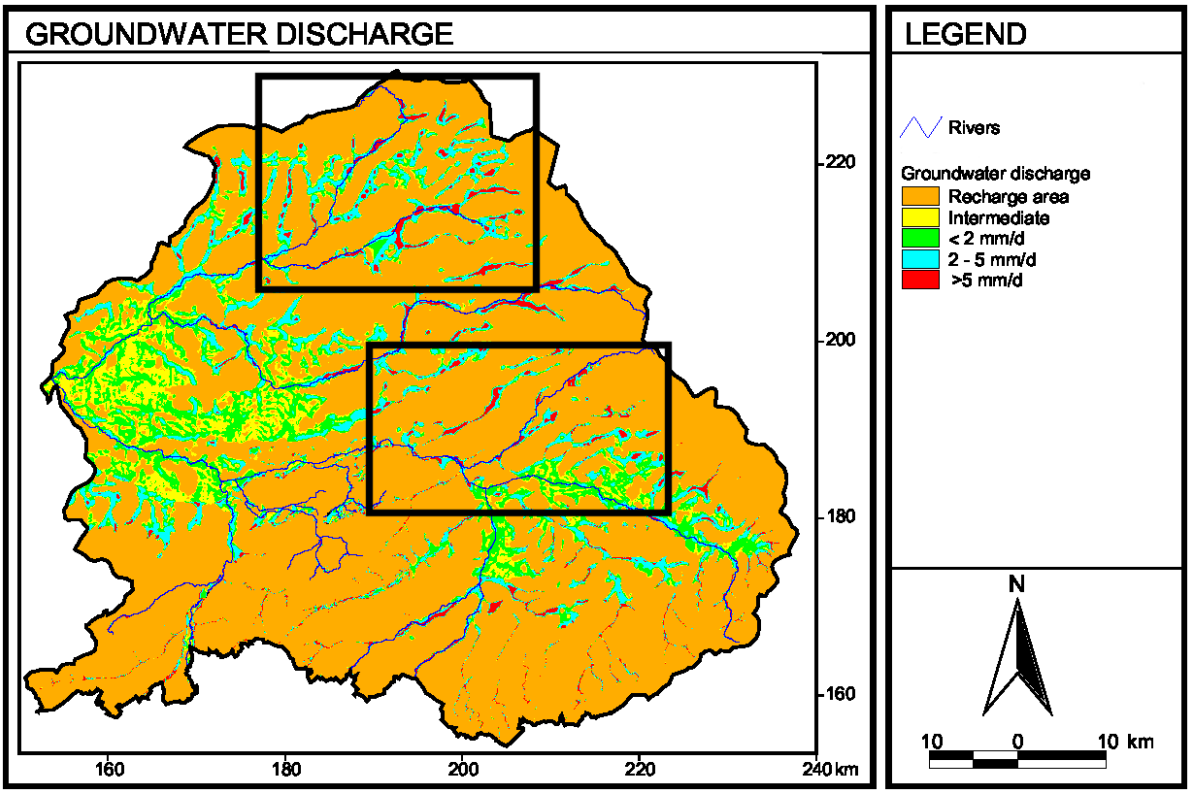

Figure S 4: Groundwater discharge and recharge in the study area, calculated using the SEEPAGE package of MODFLOW[6] (picture adapted from ref.[3]). The black rectangles indicate the study area and agree with the maps in Figure S 1. Along most stretches of the streams of the studied catchments, the model predicts that groundwater is discharged into the streams.

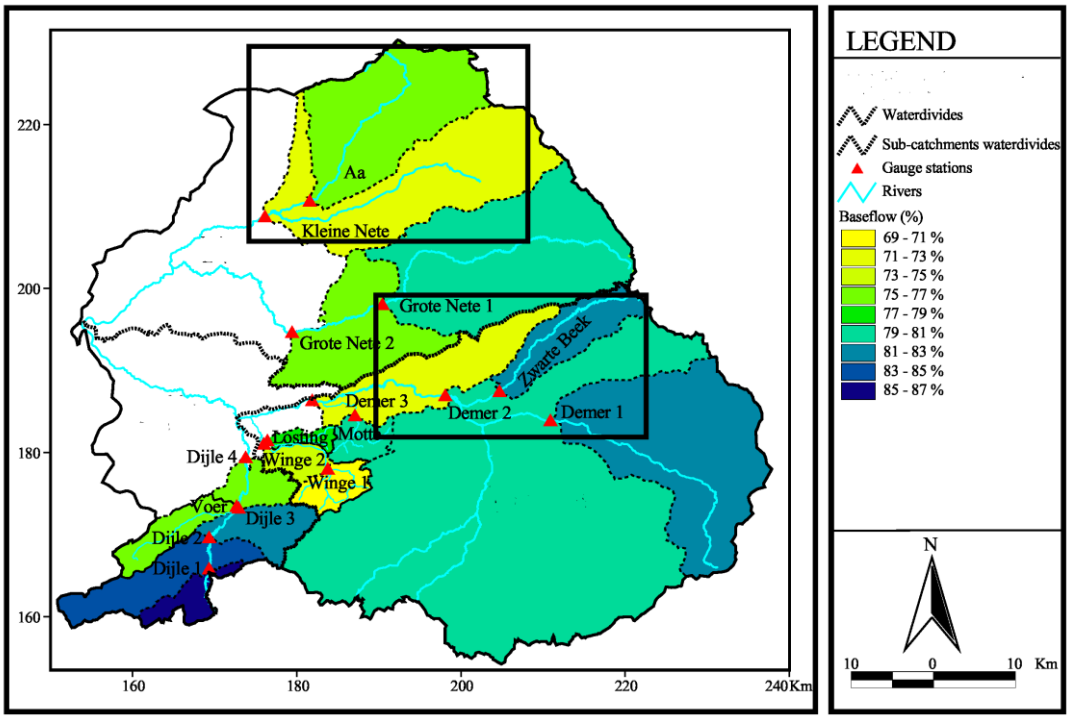

Figure S 5: Baseflow contribution to stream flow, calculated from the total hydrograph by numerical discharge separation (adapted from ref. [3]). These data result from hydrograph analysis of 17 river gauging stations, each with at least 10 years of daily discharge data available. The black rectangles indicate the study area and agree with the maps in Figure S 1. The baseflow contribution in subcatchments of the study area ranges between 71 and 83%.

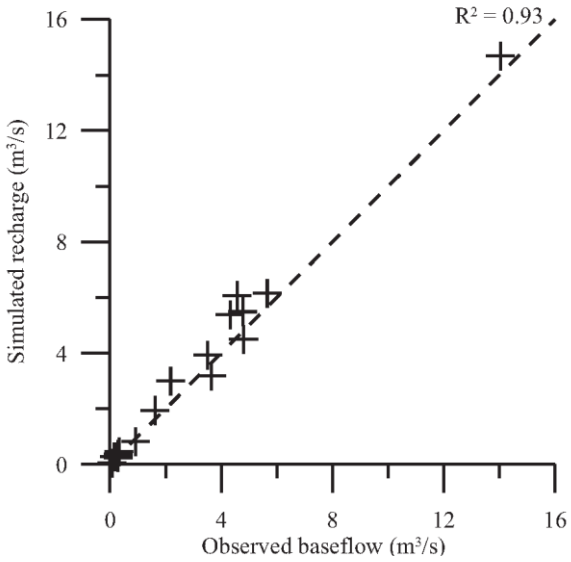

Figure S 6: Correlation between the simulated groundwater recharge, calculated with the WetSpass model (Figure S 3), and the observed baseflow in the 17 subcatchments shown in Figure S 5 (adapted from ref. [3]).

2. Methodological details

Measurement of characteristics and composition of groundwater and surface water

The pH, water temperature, O_2 concentration, and electrical conductivity (EC) were measured in the field using field electrodes (WTW pH/Oxi 340i and Mettler Toledo FiveGo). Groundwater and surface water samples were membrane filtered in the field (0.45 µm Chromafil Xtra PET 45/25 filters), and subsamples were immediately acidified (HCl, final concentration 0.01 M) in order to stabilize the oxidation state of Fe. The dissolved organic carbon (DOC) concentration was measured as the non-purgeable organic carbon on an elemental analyzer (AnalytikJena, Multi N/C 2100), total dissolved element concentrations were measured by ICP-MS (Agilent 7700x), the dissolved Fe(II) concentration was determined colorimetrically using the ferrozine method[7], and the dissolved Fe(III) concentration was determined as the difference between the concentrations of total dissolved Fe (ICP-MS) and dissolved Fe(II) (colorimetry). The dissolved concentrations of anions (Cl^-, SO_4^{2-}, NO_3^-) and inorganic carbon (DIC) were determined in selected samples by anion chromatography (Dionex ICS-2000 with AS18 column) and by an elemental analyzer (AnalytikJena, Multi N/C 2100), respectively. All concentrations in this study were determined after membrane filtration (0.45 µm) and are referred to as "dissolved" concentrations.

Suspended sediment samples

At selected locations, suspended sediment samples were isolated from streamwater by vacuum filtration over a 0.45 µm nitrocellulose filter membrane. The suspended sediment was dried at 60°C, and the concentrations of Fe, P, and As were determined by ICP-OES (Perkin Elmer, Optima 3300 DV) after extraction with boiling *aqua regia* (50 mg suspended sediment in 2 mL *aqua regia* heated in a hot block at 140°C for 2 h).

Estimation of water flow velocity

In order to estimate the hydraulic residence time of the water (see main manuscript), the water flow velocity in each stream stretch of the studied catchments and at each sampling moment was estimated. The starting point of flow velocity calculations was the typical year-averaged flow velocity in each stream class[8], whereby the class of each stream stretch was derived from the hydrographic atlas of the Flanders region[9]. These typical year-averaged flow velocities were then converted to values specific for each sampling moment using data obtained by 8

permanent flow velocity loggers installed at various locations in the studied catchments. For each stream stretch, a flow velocity logger at a nearby location and in a stream of similar size was selected. From the permanent flow velocity monitoring dataset, the ratio of the flow velocity measured during each of four sampling moments divided by the year-averaged flow velocity was calculated. Finally, multiplication of this ratio with the typical year-averaged flow velocity (estimated based on the stream class) yielded the estimated flow velocity in each stream stretch and at each sampling moment.

3. Characteristics and composition of groundwater and streams

Table S 1: Characteristics and concentrations of selected elements in filtered (0.45 µm) groundwater and streamwater samples.

		pH	temp	O_2	EC	Fe	Fe(II)	Na	Mg	Al	P	Ca	Cr	Mn	Co	Ni	Cu	Zn	As	Pb	DOC
			°C	*mg/L*	*µS/cm*	*mg/L*	*mg/L*	*mg/L*	*mg/L*	*µg/L*	*µg/L*	*mg/L*	*µg/L*	*µg/L*	*µg/L*	*µg/L*	*µg/L*	*µg/L*	*µg/L*	*µg/L*	*mg/L*
Groundwater	**Min**	4.8	5.9	0.6	119	0.4	< 0.02	3	0.7	2	3	5	0.05	9	0.04	0.1	< 0.1	2.1	0.3	0.03	1.3
	P_{10}	5.6	7.9	1.0	192	3.9	3.0	5	1.2	4	24	11	0.1	25	0.1	0.2	0.1	3.3	1.0	0.05	3.0
	Median	6.3	11.7	1.4	469	13.2	13.9	15	4.2	15	203	37	0.4	167	0.2	0.8	0.5	6.4	6.1	0.18	7.8
	P_{90}	6.8	16.2	2.3	799	44.5	45.0	55	8.6	124	938	72	2.5	773	6.4	8.7	1.9	24.4	36.0	0.60	18.9
	Max	7.2	20.7	9.6	1780	91.5	97.5	202	35.3	1778	2611	131	43.8	3346	30.4	47.9	33.0	253.4	294.3	28.64	42.4
	Mean	6.2	12.0	1.6	491	19.5	20.5	24	4.9	77	393	38	1.2	295	2.0	3.2	1.3	12.3	16.5	0.55	10.0
	Stdev	0.5	3.1	0.9	256	17.8	19.4	26	4.1	226	528	26	3.6	456	4.7	6.8	3.8	22.0	35.2	2.47	8.4
	N	162	163	163	155	162	136	162	162	162	160	162	162	162	162	162	162	162	162	162	160
Streams	**Min**	4.3	3.0	1.6	75	0.08	0.02	4	1.5	1	2	9	0.1	5	0.1	0.4	0.1	1.7	0.3	0.01	2.3
	P_{10}	6.1	6.6	4.8	264	0.2	0.08	11	2.9	5	11	21	0.1	31	0.4	1.2	0.3	7.3	0.6	0.07	4.2
	Median	6.6	12.9	6.8	415	1.0	0.5	23	5.4	12	33	34	0.3	125	1.4	3.4	0.9	16.5	1.1	0.19	7.4
	P_{90}	7.0	17.9	9.6	683	6.1	4.4	53	7.4	51	79	56	0.7	233	6.1	8.0	2.2	51.7	2.5	0.47	11.8
	Max	8.2	23.9	14.7	1800	70.2	74.6	127	31.4	162	374	112	1.2	539	13.3	28.4	6.6	203.3	10.3	2.96	29.7
	Mean	6.6	12.1	6.9	458	3.6	2.9	28	5.6	23	42	37	0.4	136	2.4	4.2	1.2	25.0	1.4	0.24	7.8
	Stdev	0.5	4.6	1.9	198	9.2	9.1	19	3.4	27	38	15	0.2	91	2.9	3.3	0.9	26.0	1.1	0.27	3.8
	N	194	195	195	189	194	187	196	196	196	194	196	196	196	196	196	196	196	196	196	194

min: lowest observed value; P_{10}: 10^{th} percentile; P_{90}: 90^{th} percentile; max: highest observed value; stdev: standard deviation; N: number of observations; temp: water temperature; EC: electrical conductivity; DOC: dissolved organic carbon

4. Variable clustering and correlation analyses

Variable clustering and correlation analyses were performed in order to better understand the relationships and associations between different variables in groundwater and streams. These analyses were performed on log-transformed variables, except for pH and temperature. The variable clustering analysis (VARCLUS procedure in SAS 9.3, SAS Institute, Cary, USA) shows which groups of variables are strongly associated with each other. This approach was preferred to more traditional ones such as principal component analysis, since the results of the variable clustering analysis are more easily interpreted. VARCLUS divides a set of variables into hierarchical clusters of variables in such a way that the variance explained by the first principal components of the variables in each cluster is maximized. The amount of clusters was set to three (for groundwater) and four (for streamwater) which yielded readily interpretable results. More details on VARCLUS can be found in the SAS/STAT 12.1 User's Guide, Chapter 100 (SAS Institute, Cary, USA). The DIC, Cl, and SO_4 concentrations were not included in the variable clustering analysis: they were only determined in selected samples, and the VARCLUS algorithm only includes samples for which all variables have been measured.

For the correlation analysis, Pearson correlation coefficients were calculated by JMP Pro 11 (SAS Institute, Cary, USA). However, statistical significance was not useful as a criterion for relevance because even at the 99% confidence limit, more than half of all correlations would be considered relevant. Therefore, a combination of a visual inspection of the correlation plots and an indicative limit of +/- 0.40 was proposed as a reasonable choice for roughly separating the relevant correlations.

Table S 2 shows the results of the variable clustering analysis for groundwater (left) and streams (right). The R^2_{own} and R^2_{next} indicate how well each variable is associated with its own cluster and with the next cluster. A high R^2_{own} indicates a strong association of a variable with its own cluster. A low $(1-R^2_{own})/(1-R^2_{next})$ ratio indicates good clustering. Relatively good clustering is obtained with only three clusters for both the groundwater and the streamwater datasets. In groundwater, cluster 1 consists of most cationic trace elements. Cluster 2 contains the electrical conductivity, the major cations, DOC, and Mn. Cluster 3 contains P, As, and Fe. The pH, temperature, and the concentrations of Si, Mo, Cd, and O_2 were only weakly associated with any cluster. The correlation analysis (Table S 3) largely confirms this clustering of variables: correlation coefficients of variables in the same cluster are generally

above 0.4 or below -0.4. The DIC, Cl, and SO_4 concentrations, which were not included in the variable clustering analysis, appear mostly associated with the variables in cluster 1, *i.e.* with the electrical conductivity and the major cations. Bivariate plots of the groundwater Fe concentrations versus those of P, As, and Mn are shown in Figure S 7. These correlations suggest that Fe may be supplied to the groundwater by a reductive dissolution reaction mechanism.

In streams, the variable clustering analysis shows one cluster with the major cations, and two other clusters which contain most trace metals and the DOC. These observations are along the same lines as those for groundwater. However, contrary to groundwater, Fe in streams is mostly associated with Mn, the streamwater temperature, and the residence time of the water. The correlation analysis (Table S 4) largely confirms these observations: within each cluster, correlation coefficients are mostly above 0.4 or below -0.4 as expected. The correlation analysis additionally shows that the streamwater temperature, which may reflect seasonal effects, is negatively correlated with many elements including Fe, Al, Cr, Mn, and Zn.

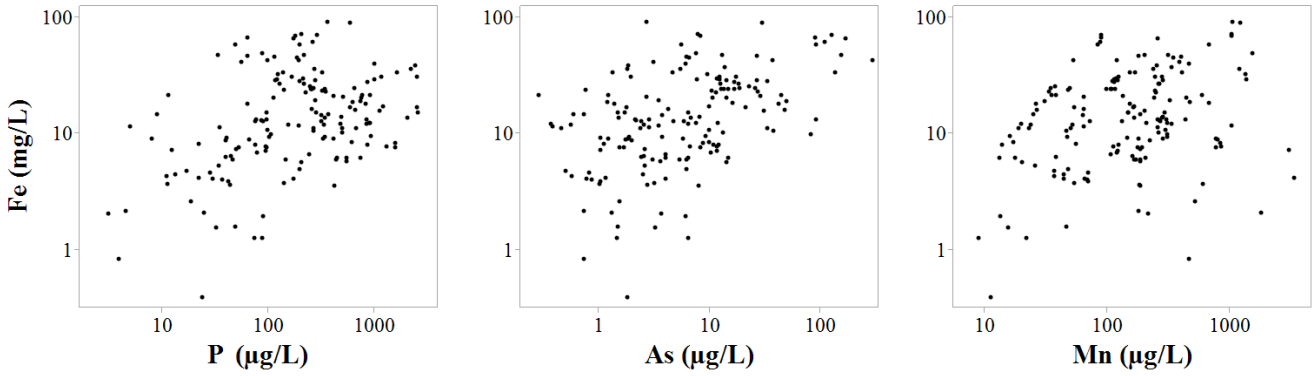

Figure S 7: Bivariate plots of the Fe concentrations in groundwater versus those of P (r = 0.42), As (r = 0.48), and Mn (r = 0.31). These correlations hint at a reductive dissolution reaction mechanism which supplies these elements to the groundwater.

Table S 2: Results of the variable clustering analysis. Variables poorly associated with any cluster ($R^2_{own} < 0.4$) are shown in gray.

GROUNDWATER

		R^2_{own}	R^2_{next}	Ratio
Cluster 1	Al	0.66	0.08	0.37
	Ni	0.60	0.18	0.48
	Pb	0.59	0.01	0.42
	Co	0.56	0.14	0.51
	Zn	0.55	0.14	0.52
	Cu	0.54	0.12	0.52
	Cr	0.54	0.01	0.47
	Cd	*0.35*	*0.05*	*0.68*
	Si	*0.18*	*0.03*	*0.85*
Cluster 2	EC	0.84	0.07	0.17
	Mg	0.72	0.01	0.28
	Ca	0.54	0.12	0.52
	K	0.52	0.03	0.49
	Na	0.46	0.13	0.62
	DOC	0.45	0.08	0.59
	Mn	0.40	0.06	0.63
Cluster 3	P	0.55	0.15	0.53
	As	0.55	0.06	0.48
	Fe	0.44	0.06	0.60
	pH	*0.37*	*0.11*	*0.71*
	Mo	*0.12*	*0.05*	*0.92*
	O_2	*0.08*	*0.01*	*0.93*
	temp	*0.02*	*0.00*	*0.98*

STREAMS

		R^2_{own}	R^2_{next}	Ratio
Cluster 1	Ca	0.75	0.23	0.32
	EC	0.72	0.11	0.31
	K	0.71	0.38	0.47
	Na	0.64	0.21	0.46
	Mg	0.63	0.13	0.42
Cluster 2	Ni	0.70	0.14	0.34
	Co	0.70	0.19	0.38
	Cd	0.64	0.21	0.45
	Al	0.64	0.29	0.51
	Cr	0.64	0.29	0.51
	Zn	0.41	0.12	0.67
	O_2	*0.09*	*0.04*	*0.95*
Cluster 3	Fe	0.71	0.06	0.31
	Mn	0.70	0.19	0.38
	res. time	0.62	0.13	0.44
	temp	0.55	0.29	0.63
	Si	0.45	0.08	0.60
	As	*0.21*	*0.03*	*0.81*
Cluster 4	Pb	0.71	0.25	0.39
	DOC	0.65	0.21	0.44
	Cu	0.59	0.28	0.56
	P	0.48	0.03	0.53
	Mo	0.46	0.29	0.76
	pH	*0.22*	*0.06*	*0.83*

EC: electrical conductivity; temp: temperature; res. time: residence time;

ratio = $(1-R^2_{own})/(1-R^2_{next})$

Table S 3: Pearson correlation coefficients for groundwater samples. All variables were log-transformed, except pH and temperature. Coefficients above 0.4 or below -0.4 are shown in yellow; coefficients above 0.6 or below -0.6 are shown in green.

	pH	temp	O2	cond	Fe	Fe(II)	Na	Mg	Al	Si	P	K	Ca	Cr	Mn	Co	Ni	Cu	Zn	As	Mo	Cd	Pb	DOC	DIC	Cl	SO4
pH	1.00	-0.14	-0.04	0.29	0.17	0.15	0.12	0.11	-0.28	0.10	0.34	-0.10	0.40	-0.23	-0.08	-0.22	-0.27	-0.11	-0.30	0.22	0.28	-0.04	-0.07	0.08	0.42	0.12	-0.07
temp	-0.14	1.00	-0.18	0.01	-0.04	0.02	0.01	-0.02	-0.04	-0.03	0.17	0.00	0.04	-0.03	0.01	-0.11	-0.11	-0.19	-0.01	0.14	0.00	-0.24	-0.20	0.06	0.10	0.00	-0.08
O2	-0.04	-0.18	1.00	0.13	-0.06	-0.07	0.14	0.09	-0.09	0.15	-0.13	-0.04	0.12	-0.03	0.09	0.12	0.04	0.06	0.22	-0.14	0.00	0.22	-0.08	0.05	0.14	0.36	0.27
cond	0.29	0.01	0.13	1.00	0.19	0.13	0.67	0.73	-0.15	0.02	0.12	0.54	0.77	-0.02	0.44	0.17	0.23	-0.07	-0.13	0.19	0.28	0.11	-0.09	0.56	0.45	0.82	0.40
Fe	0.17	-0.04	-0.06	0.19	1.00	0.98	-0.08	0.14	-0.18	0.32	0.42	-0.06	0.10	0.09	0.31	-0.18	-0.24	-0.32	-0.19	0.48	-0.05	-0.22	-0.06	0.19	-0.15	0.20	0.13
Fe(II)	0.15	0.02	-0.07	0.13	0.98	1.00	-0.13	0.16	-0.20	0.37	0.48	-0.05	0.09	0.08	0.31	-0.18	-0.22	-0.32	-0.21	0.50	-0.04	-0.24	-0.09	0.10	-0.14	0.20	0.09
Na	0.12	0.01	0.14	0.67	-0.08	-0.13	1.00	0.35	0.24	-0.21	-0.01	0.38	0.30	0.32	0.43	0.39	0.43	0.14	0.06	0.00	0.34	0.21	0.16	0.59	0.18	0.71	0.57
Mg	0.11	-0.02	0.09	0.73	0.14	0.16	0.35	1.00	-0.20	-0.02	0.00	0.67	0.72	-0.06	0.45	0.15	0.33	-0.10	-0.14	0.10	0.10	0.12	-0.15	0.41	0.24	0.72	0.32
Al	-0.28	-0.04	-0.09	-0.15	-0.18	-0.20	0.24	-0.20	1.00	-0.31	-0.29	-0.05	-0.39	0.78	0.15	0.47	0.51	0.45	0.46	-0.17	0.02	0.27	0.74	0.20	-0.06	0.14	0.35
Si	0.10	-0.03	0.15	0.02	0.32	0.37	-0.21	-0.02	-0.31	1.00	0.30	0.03	0.16	-0.12	-0.07	-0.25	-0.36	-0.26	-0.16	0.05	-0.33	-0.05	-0.26	0.04	0.28	0.02	-0.07
P	0.34	0.17	-0.13	0.12	0.42	0.48	-0.01	0.00	-0.29	0.30	1.00	-0.13	0.23	-0.07	-0.08	-0.46	-0.41	-0.25	-0.30	0.33	0.21	-0.19	-0.13	0.05	0.38	0.07	-0.17
K	-0.10	0.00	-0.04	0.54	-0.06	-0.05	0.38	0.67	-0.05	0.03	-0.13	1.00	0.36	0.07	0.56	0.39	0.52	0.06	0.04	-0.06	0.10	0.27	0.01	0.32	0.05	0.71	0.46
Ca	0.40	0.04	0.12	0.77	0.10	0.09	0.30	0.72	-0.39	0.16	0.23	0.36	1.00	-0.32	0.21	-0.20	-0.10	-0.21	-0.34	0.18	0.19	-0.03	-0.29	0.38	0.54	0.53	0.05
Cr	-0.23	-0.03	-0.03	-0.02	0.09	0.08	0.32	-0.06	0.78	-0.12	-0.07	0.07	-0.32	1.00	0.27	0.50	0.57	0.34	0.42	-0.07	0.05	0.27	0.64	0.44	0.10	0.19	0.04
Mn	-0.08	0.01	0.09	0.44	0.31	0.31	0.43	0.45	0.15	-0.07	-0.08	0.56	0.21	0.27	1.00	0.34	0.39	0.11	0.06	0.00	0.12	0.18	0.11	0.32	-0.27	0.54	0.64
Co	-0.22	-0.11	0.12	0.17	-0.18	-0.18	0.39	0.15	0.47	-0.25	-0.46	0.39	-0.20	0.50	0.34	1.00	0.82	0.41	0.51	-0.15	0.02	0.52	0.40	0.33	-0.19	0.41	0.33
Ni	-0.27	-0.11	0.04	0.23	-0.24	-0.22	0.43	0.33	0.51	-0.36	-0.41	0.52	-0.10	0.57	0.39	0.82	1.00	0.49	0.46	-0.21	0.16	0.46	0.45	0.38	-0.15	0.39	0.30
Cu	-0.11	-0.19	0.06	-0.07	-0.32	-0.32	0.14	-0.10	0.45	-0.26	-0.25	0.06	-0.21	0.34	0.11	0.41	0.49	1.00	0.61	-0.30	0.21	0.52	0.57	0.01	-0.13	-0.24	-0.04
Zn	-0.30	-0.01	0.22	-0.13	-0.19	-0.21	0.06	-0.14	0.46	-0.16	-0.30	0.04	-0.34	0.42	0.06	0.51	0.46	0.61	1.00	-0.26	-0.02	0.60	0.53	0.04	-0.52	-0.06	0.18
As	0.22	0.14	-0.14	0.19	0.48	0.50	0.00	0.10	-0.17	0.05	0.33	-0.06	0.18	-0.07	0.00	-0.15	-0.21	-0.30	-0.26	1.00	0.19	-0.18	-0.08	0.17	0.26	0.07	-0.33
Mo	0.28	0.00	0.00	0.28	-0.05	-0.04	0.34	0.10	0.02	-0.33	0.21	0.10	0.19	0.05	0.12	0.02	0.16	0.21	-0.02	0.19	1.00	0.10	0.18	0.17	0.25	-0.06	-0.21
Cd	-0.04	-0.24	0.22	0.11	-0.22	-0.24	0.21	0.12	0.27	-0.05	-0.19	0.27	-0.03	0.27	0.18	0.52	0.46	0.52	0.60	-0.18	0.10	1.00	0.38	0.19	-0.16	0.19	0.17
Pb	-0.07	-0.20	-0.08	-0.09	-0.06	-0.09	0.16	-0.15	0.74	-0.26	-0.13	0.01	-0.29	0.64	0.11	0.40	0.45	0.57	0.53	-0.08	0.18	0.38	1.00	0.10	-0.05	-0.12	0.12
DOC	0.08	0.06	0.05	0.56	0.19	0.10	0.59	0.41	0.20	0.04	0.05	0.32	0.38	0.44	0.32	0.33	0.38	0.01	0.04	0.17	0.17	0.19	0.10	1.00	0.50	0.54	0.08
DIC	0.42	0.10	0.14	0.45	-0.15	-0.14	0.18	0.24	-0.06	0.28	0.38	0.05	0.54	0.10	-0.27	-0.19	-0.15	-0.13	-0.52	0.26	0.25	-0.16	-0.05	0.50	1.00	0.12	-0.34
Cl	0.12	0.00	0.36	0.82	0.20	0.20	0.71	0.72	0.14	0.02	0.07	0.71	0.53	0.19	0.54	0.41	0.39	-0.24	-0.06	0.07	-0.06	0.19	-0.12	0.54	0.12	1.00	0.49
SO4	-0.07	-0.08	0.27	0.40	0.13	0.09	0.57	0.32	0.35	-0.07	-0.17	0.46	0.05	0.04	0.64	0.33	0.30	-0.04	0.18	-0.33	-0.21	0.17	0.12	0.08	-0.34	0.49	1.00

temp: water temperature; cond: electrical conductivity; DOC: dissolved organic carbon; DIC: dissolved inorganic carbon

Table S 4: Pearson correlation coefficients for streamwater samples. All variables were log-transformed, except pH and temperature. Coefficients above 0.4 or below -0.4 are shown in yellow; coefficients above 0.6 or below -0.6 are shown in green.

	pH	temp	O2	cond	Fe	Fe(II)	Na	Mg	Al	Si	P	K	Ca	Cr	Mn	Co	Ni	Cu	Zn	As	Mo	Cd	Pb	DOC	DIC	Cl	SO4	res.time
pH	1.00	0.05	0.19	0.14	-0.27	-0.30	0.30	-0.04	-0.01	-0.20	0.26	0.19	0.25	-0.05	-0.29	-0.23	-0.02	0.21	-0.13	-0.03	0.38	-0.13	0.26	0.26	0.58	0.20	-0.34	0.17
temp	0.05	1.00	-0.21	0.06	-0.46	-0.41	0.11	-0.01	-0.42	-0.40	-0.10	-0.02	0.13	-0.44	-0.53	-0.48	-0.28	-0.03	-0.43	-0.17	0.16	-0.50	-0.25	-0.17	0.19	0.11	-0.14	0.57
O2	0.19	-0.21	1.00	0.01	-0.26	-0.22	0.18	0.13	0.14	-0.25	-0.05	0.03	0.15	0.14	-0.20	0.22	0.31	0.31	0.08	-0.25	0.17	0.17	0.15	-0.03	0.31	0.07	0.19	0.07
cond	0.14	0.06	0.01	1.00	-0.04	-0.13	0.65	0.60	0.05	0.02	0.14	0.57	0.68	0.01	0.01	0.02	0.24	0.28	0.14	-0.09	0.36	0.07	0.20	0.24	-0.22	0.66	0.69	0.22
Fe	-0.27	-0.46	-0.26	-0.04	1.00	0.95	-0.41	0.01	0.21	0.42	-0.08	-0.24	-0.26	0.19	0.61	0.32	-0.01	-0.21	0.23	0.55	-0.50	0.37	-0.02	-0.03	-0.54	0.04	0.31	-0.54
Fe(II)	-0.30	-0.41	-0.22	-0.13	0.95	1.00	-0.48	-0.10	0.17	0.41	-0.13	-0.27	-0.28	0.16	0.51	0.29	-0.07	-0.19	0.21	0.54	-0.56	0.34	-0.06	-0.12	-0.50	-0.09	0.20	-0.49
Na	0.30	0.11	0.18	0.65	-0.41	-0.48	1.00	0.44	0.04	-0.19	0.24	0.67	0.58	0.00	-0.27	-0.11	0.24	0.34	0.01	-0.26	0.64	-0.08	0.22	0.28	0.42	0.67	0.12	0.40
Mg	-0.04	-0.01	0.13	0.60	0.01	-0.10	0.44	1.00	0.26	-0.11	-0.06	0.56	0.69	0.07	0.11	0.34	0.45	0.29	0.07	-0.12	0.22	0.33	0.18	0.19	-0.37	0.51	0.94	0.20
Al	-0.01	-0.42	0.14	0.05	0.21	0.17	0.04	0.26	1.00	-0.16	0.38	0.30	0.09	0.70	0.27	0.52	0.55	0.48	0.39	0.25	0.15	0.61	0.64	0.48	-0.46	0.12	0.36	-0.28
Si	-0.20	-0.40	-0.25	0.02	0.42	0.41	-0.19	-0.11	-0.16	1.00	-0.02	-0.10	-0.05	0.04	0.57	0.10	-0.18	-0.26	0.17	0.09	-0.39	0.14	-0.15	-0.05	-0.30	-0.25	0.05	-0.34
P	0.26	-0.10	-0.05	0.14	-0.08	-0.13	0.24	-0.06	0.38	-0.02	1.00	0.36	0.11	0.37	-0.10	-0.14	0.09	0.30	0.01	0.15	0.45	0.03	0.50	0.50	0.37	0.17	-0.37	-0.04
K	0.19	-0.02	0.03	0.57	-0.24	-0.27	0.67	0.56	0.30	-0.10	0.36	1.00	0.66	0.29	-0.09	0.12	0.39	0.52	0.20	-0.10	0.46	0.14	0.41	0.56	0.05	0.45	0.33	0.22
Ca	0.25	0.13	0.15	0.68	-0.26	-0.28	0.58	0.69	0.09	-0.05	0.11	0.66	1.00	0.01	-0.12	-0.03	0.19	0.49	0.01	-0.13	0.49	0.17	0.28	0.34	0.07	0.66	0.70	0.28
Cr	-0.05	-0.44	0.14	0.01	0.19	0.16	0.00	0.07	0.70	0.04	0.37	0.29	0.01	1.00	0.40	0.52	0.55	0.47	0.38	0.14	0.02	0.50	0.52	0.69	0.06	-0.16	0.08	-0.33
Mn	-0.29	-0.53	-0.20	0.01	0.61	0.51	-0.27	0.11	0.27	0.57	-0.10	-0.09	-0.12	0.40	1.00	0.59	0.25	-0.10	0.37	0.14	-0.39	0.37	0.07	0.11	-0.55	-0.20	0.44	-0.61
Co	-0.23	-0.48	0.22	0.02	0.32	0.29	-0.11	0.34	0.52	0.10	-0.14	0.12	-0.03	0.52	0.59	1.00	0.77	0.21	0.48	0.08	-0.23	0.59	0.21	0.13	-0.55	0.13	0.72	-0.32
Ni	-0.02	-0.28	0.31	0.24	-0.01	-0.07	0.24	0.45	0.55	-0.18	0.09	0.39	0.19	0.55	0.25	0.77	1.00	0.44	0.47	-0.16	0.20	0.52	0.34	0.35	-0.24	0.39	0.62	-0.11
Cu	0.21	-0.03	0.31	0.28	-0.21	-0.19	0.34	0.29	0.48	-0.26	0.30	0.52	0.49	0.47	-0.10	0.21	0.44	1.00	0.30	-0.06	0.38	0.44	0.62	0.55	0.12	0.11	0.14	0.04
Zn	-0.13	-0.43	0.08	0.14	0.23	0.21	0.01	0.07	0.39	0.17	0.01	0.20	0.01	0.38	0.37	0.48	0.47	0.30	1.00	-0.04	-0.04	0.53	0.25	0.13	-0.59	-0.06	0.50	-0.33
As	-0.03	-0.17	-0.25	-0.09	0.55	0.54	-0.26	-0.12	0.25	0.09	0.15	-0.10	-0.13	0.14	0.14	0.08	-0.16	-0.06	-0.04	1.00	-0.11	0.17	0.18	0.06	-0.20	0.04	-0.09	-0.29
Mo	0.38	0.16	0.17	0.36	-0.50	-0.56	0.64	0.22	0.15	-0.39	0.45	0.46	0.49	0.02	-0.39	-0.23	0.20	0.38	-0.04	-0.11	1.00	-0.08	0.32	0.28	0.57	0.43	-0.19	0.40
Cd	-0.13	-0.50	0.17	0.07	0.37	0.34	-0.08	0.33	0.61	0.14	0.03	0.14	0.17	0.50	0.37	0.59	0.52	0.44	0.53	0.17	-0.08	1.00	0.36	0.23	-0.53	0.18	0.67	-0.40
Pb	0.26	-0.25	0.15	0.20	-0.02	-0.06	0.22	0.18	0.64	-0.15	0.50	0.41	0.28	0.52	0.07	0.21	0.34	0.62	0.25	0.18	0.32	0.36	1.00	0.61	0.20	0.26	-0.01	-0.15
DOC	0.26	-0.17	-0.03	0.24	-0.03	-0.12	0.28	0.19	0.48	-0.05	0.50	0.56	0.34	0.69	0.11	0.13	0.35	0.55	0.13	0.06	0.28	0.23	0.61	1.00	0.56	0.05	-0.17	-0.06
DIC	0.58	0.19	0.31	-0.22	-0.54	-0.50	0.42	-0.37	-0.46	-0.30	0.37	0.05	0.07	0.06	-0.55	-0.55	-0.24	0.12	-0.59	-0.20	0.57	-0.53	0.20	0.56	1.00	0.06	-0.48	0.30
Cl	0.20	0.11	0.07	0.66	0.04	-0.09	0.67	0.51	0.12	-0.25	0.17	0.45	0.66	-0.16	-0.20	0.13	0.39	0.11	-0.06	0.04	0.43	0.18	0.26	0.05	0.06	1.00	0.44	0.09
SO4	-0.34	-0.14	0.19	0.69	0.31	0.20	0.12	0.94	0.36	0.05	-0.37	0.33	0.70	0.08	0.44	0.72	0.62	0.14	0.50	-0.09	-0.19	0.67	-0.01	-0.17	-0.48	0.44	1.00	-0.02
res. time	0.17	0.57	0.07	0.22	-0.54	-0.49	0.40	0.20	-0.28	-0.34	-0.04	0.22	0.28	-0.33	-0.61	-0.32	-0.11	0.04	-0.33	-0.29	0.40	-0.40	-0.15	-0.06	0.30	0.09	-0.02	1.00

temp: water temperature; cond: electrical conductivity; DOC: dissolved organic carbon; DIC: dissolved inorganic carbon; res. time: hydrological residence time

5. Effects of seasonality and geology on the Fe concentrations in groundwater

The effects of seasonality and geology on the dissolved Fe concentrations in groundwater are examined in detail in this section. An ANOVA model for the (log-transformed) Fe concentrations in groundwater was constructed with sampling location and sampling month as the factors (Table S 5). Both had significant effects with P-values of 0.002 for sampling month and 10^{-28} for the sampling location. The sampling location is strongly related to the Fe concentration in groundwater, whereas the influence of seasonality appears limited: sampling location explains a much larger part of the variability than sampling month. Moreover, the means of the Fe concentrations sampled in different months differ by no more than 50%. The limited effect of seasonality on groundwater Fe concentrations also becomes evident from Figure S 8.

Since the Fe concentrations in groundwater strongly depend on the sampling location, the local geology could be an explaining factor for the Fe concentrations in groundwater. In particular, it has been suggested that the geological Formation of Diest, due to its high glauconite content and high permeability, supplies most of the Fe to the studied streams[10]. In order to test this hypothesis, the geological units present at a certain depth below the surface were calculated. Two different depths were used: 4 m, the depth of the groundwater monitoring wells, and a deeper depth of 10 m. The geological data were calculated from G3Dv2, the Geological Model of Flanders and Brussels[11] (publicly available at https://dov.vlaanderen.be/), and maps were constructed with the QGIS Geographic Information System (available at http://qgis.osgeo.org). Statistical analyses were carried out on log transformed data in JMP Pro 11 (SAS Institute, Cary, USA).

The groundwater Fe concentrations are plotted against the geological units present at 4 and 10 m depth (Figure S 9). Maps of the groundwater Fe concentrations (averaged over four samplings) and the geological units at 4 m depth (Figure S 10) and 10 m depth (Figure S 11) are shown. There is little association between the lithology and the Fe concentrations in groundwater. In the monitoring wells where the Formation of Diest is found at 10 m depth, the median groundwater Fe concentration is twofold larger than that in other monitoring wells. According to the Levene test, the assumption of equal variances was rejected ($P < 0.05$), and therefore no ANOVA analysis was performed. Welch's t-test shows that the mean Fe concentrations differ between the groups ($P < 0.05$). The Wilcoxon rank-sum test identifies that the Fe concentrations in groundwater where the Formation of Diest is found at

10 m depth differ from those of only three other groups ($P < 0.05$). Overall, it appears difficult to detect differences in groundwater Fe concentrations depending on the geological units, and if there are any differences, they are relatively small in magnitude. Possibly, the geological model used here is insufficiently detailed to establish a relationship between groundwater Fe concentrations and the lithology. The resolution of the model is not very high: the model units consist each of different formations, which in turn consist of different members. The aquifers in the study areas are highly heterogeneous with respect to e.g. glauconite content, hydraulic conductivity, and chemical and microbial properties which may control the glauconite weathering rate[10]. It is unclear which of these properties govern the groundwater Fe concentrations. Alternatively, the dissolved Fe in groundwater may be the integral of all Fe supplied by the geological units along the flow paths of the groundwater, and hence it may not be much related to the Fe supplied by the geological unit at the sampling location. The highly permeable and glauconite-rich Formation of Diest (greensands) occurs everywhere throughout the study areas. Its top is at most 60 m below the soil surface and it is in direct contact with the shallow unconfined aquifers. It is therefore not unlikely that the sampled groundwater once was in contact with this formation, and that the present Fe concentrations in groundwater reflect Fe supply from the past rather than Fe supply from the geological layers it is presently recovered from. In summary, the Fe concentrations in groundwater may be governed by properties of the aquifer, such as glauconite content, hydraulic conductivity, weathering rate of glauconite, and possibly also by the flow paths of the groundwater or by the presence of electron donors which reductively dissolve Fe oxyhydroxides. A more detailed survey of the lithology of the study areas may reveal which factors explain the variable Fe concentrations in groundwater, but such is beyond the scope of this study.

Table S 5: Results of the two-factor ANOVA model for the Fe concentration in groundwater.

	Sum of squares	**df**	**Mean squares**	**F**	**P**
Sampling location	24.3	51	0.48	13.5	10^{-28}
Sampling month	0.6	3	0.19	5.4	0.002
Error	3.8	107	0.04		
Total	29.0	161			

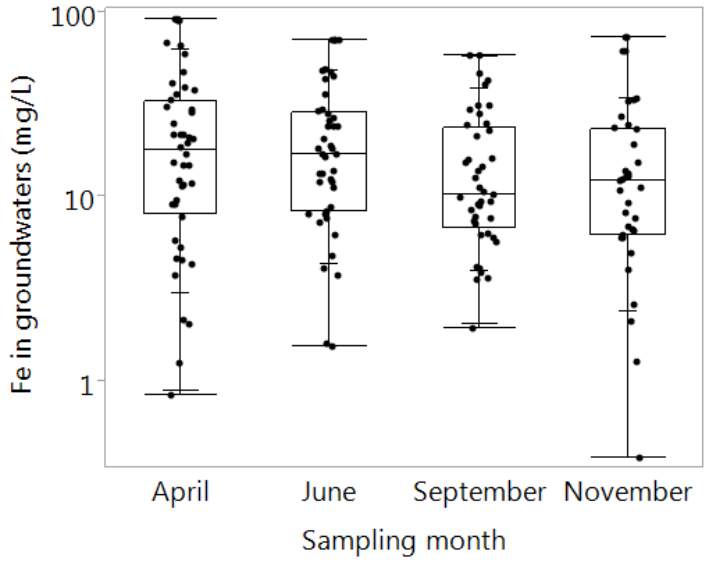

Figure S 8: Effect of seasonality on the Fe concentrations in groundwater.

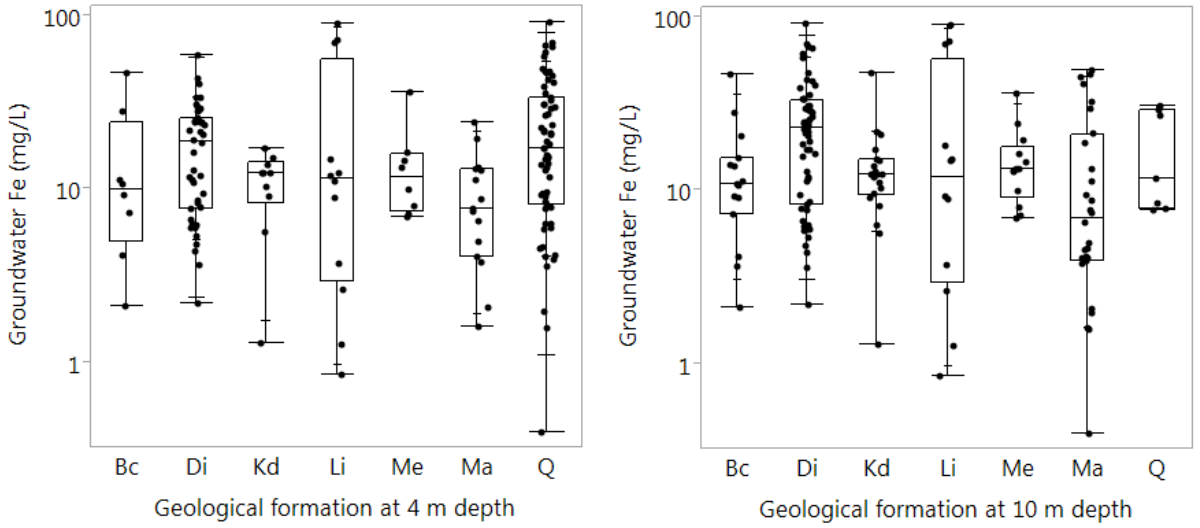

Figure S 9: Dissolved Fe concentrations in groundwater plotted against the geological formation present at 10 m below the surface. Codes of the geological formations: Bc: Berchem-Bolderberg; Di: Diest; Kd: Kattendijk-Kasterlee; Li: Lillo-Poederlee-Mol; Me: Merksplas; Ma: Malle; Q: Holocene and Middle and Late Pleistocene.

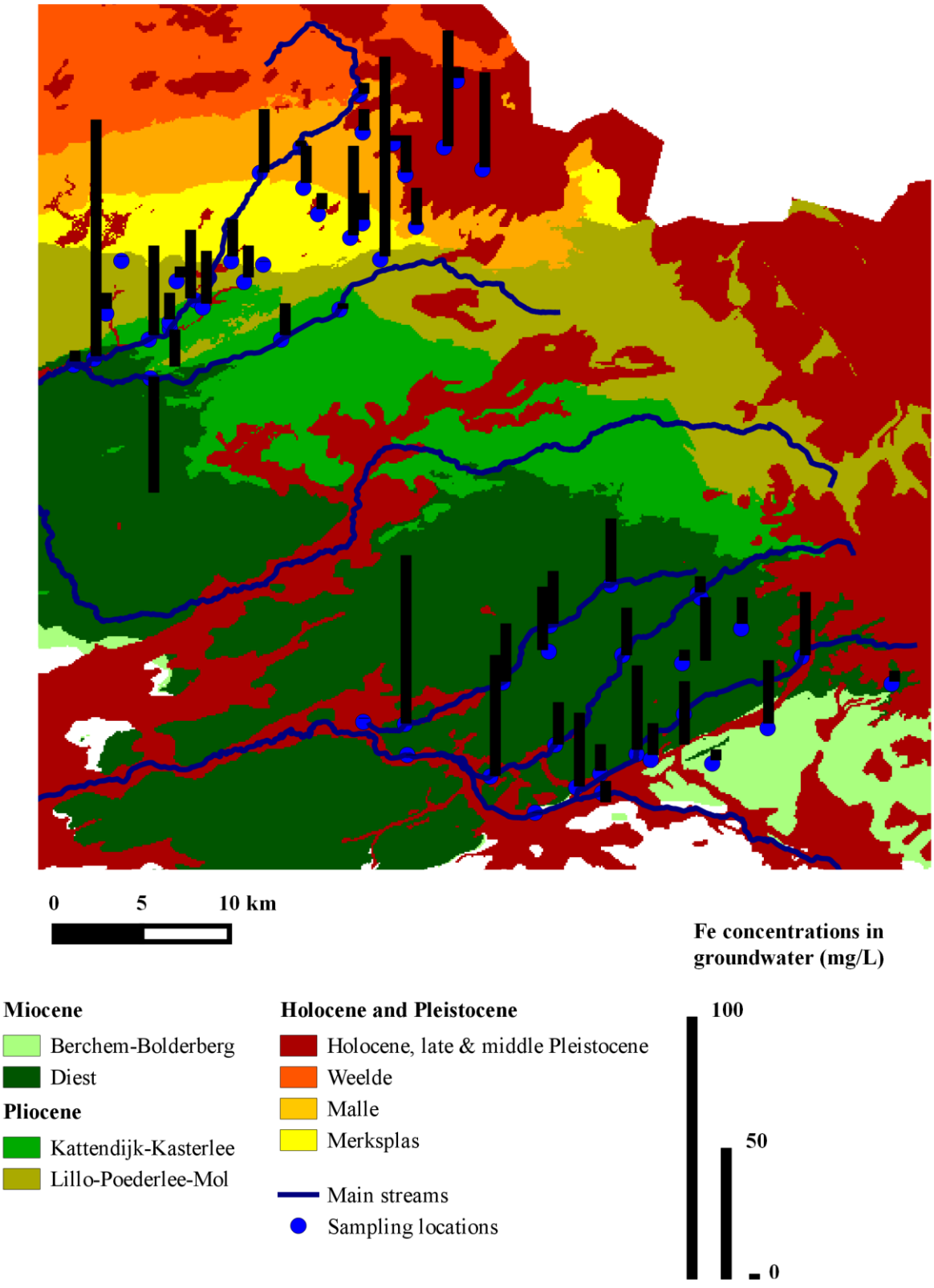

Figure S 10: Map of the dissolved Fe concentrations in groundwater (black bars; mean of four samplings) and the geological formations present at 4 m below the surface.

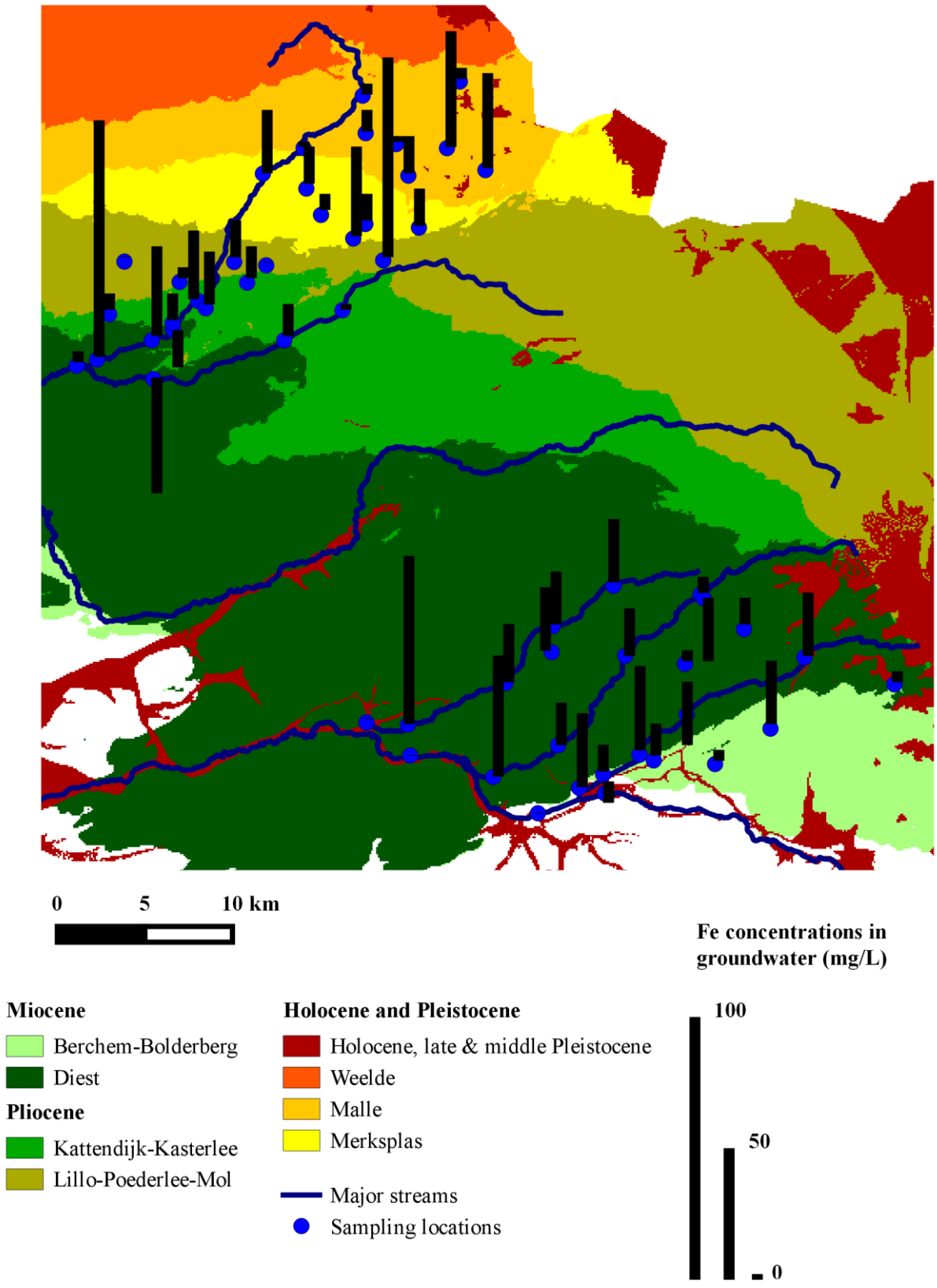

Figure S 11: Map of the dissolved Fe concentrations in groundwater (black bars; mean of four samplings) and the geological formations present at 10 m below the surface.

6. Comparison of the composition of groundwater and streams

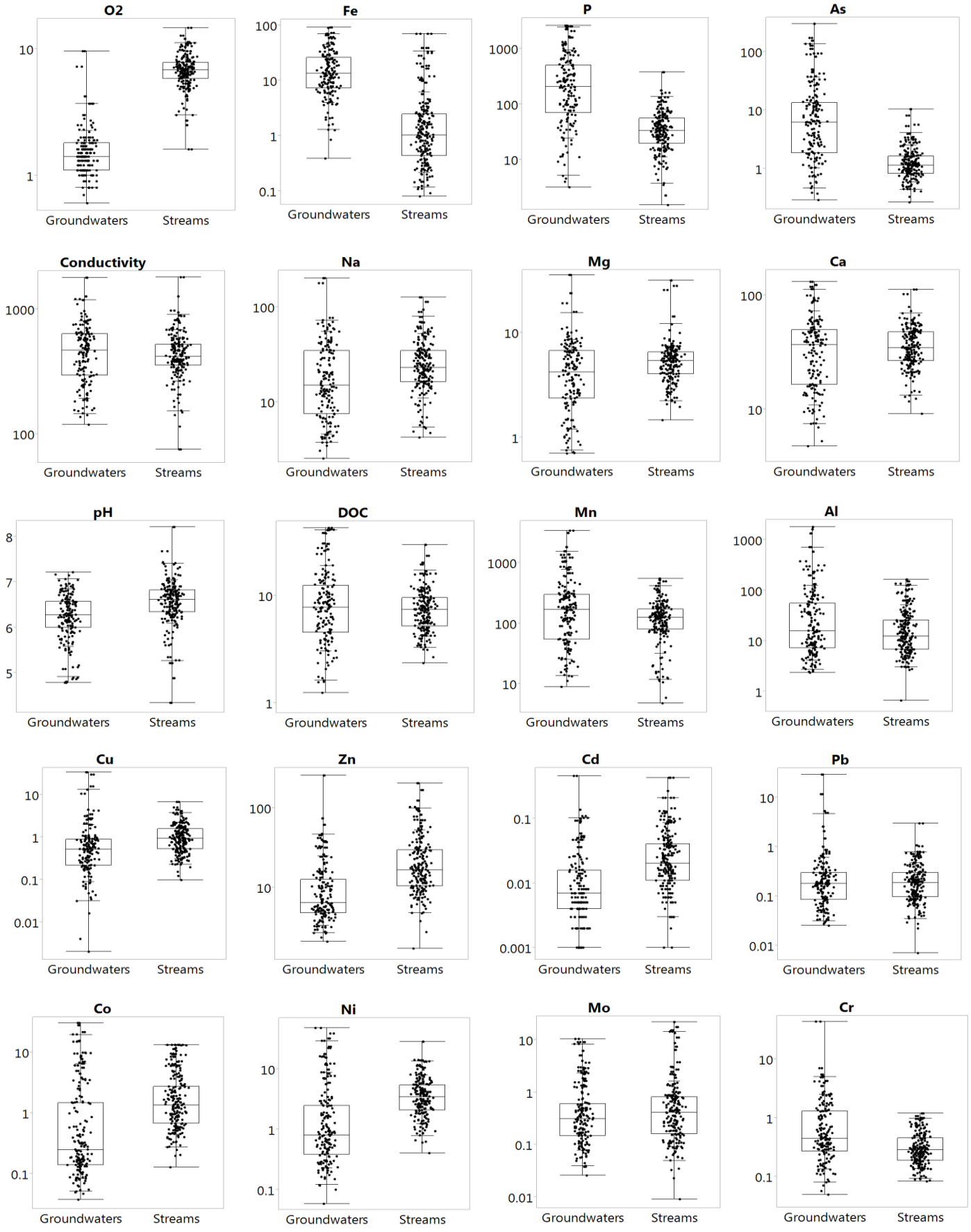

Figure S 12: The pH and concentration range of selected variables and elements in groundwater and streams. Units: µS cm^{-1} (electrical conductivity); mg L^{-1} (O_2, DOC, Na, Mg, Ca, Fe); µg L^{-1} (other elements).

7. The dissolved Fe(II) concentrations in streams

In the manuscript, we show plots of dissolved Fe concentrations in streams versus the hydrological stream order and the hydrological residence time. Figure S 13 shows similar plots but using the dissolved Fe(II) rather than the total dissolved Fe concentrations. The observed trends are similar.

A

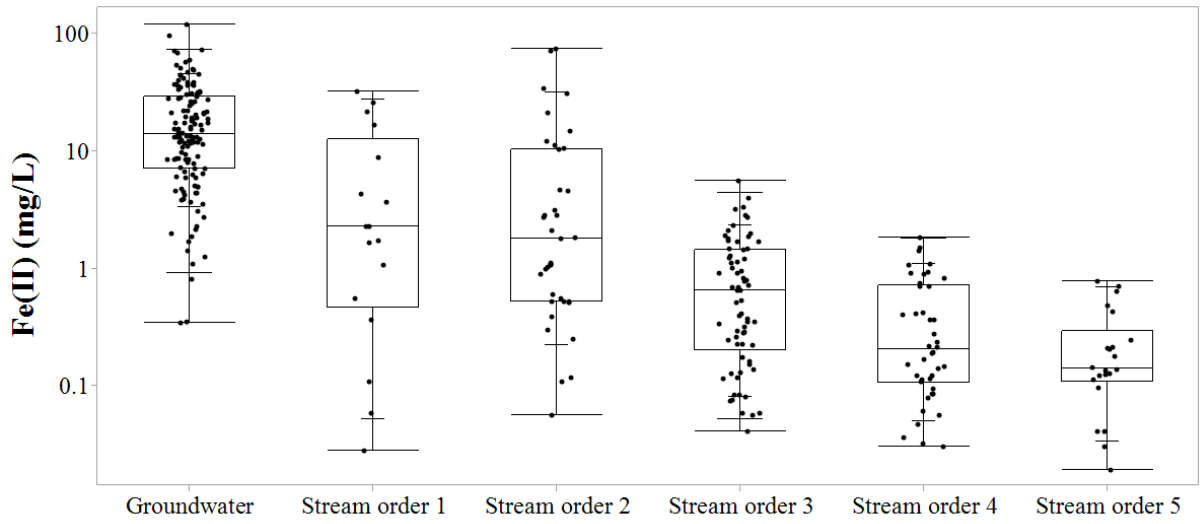

B

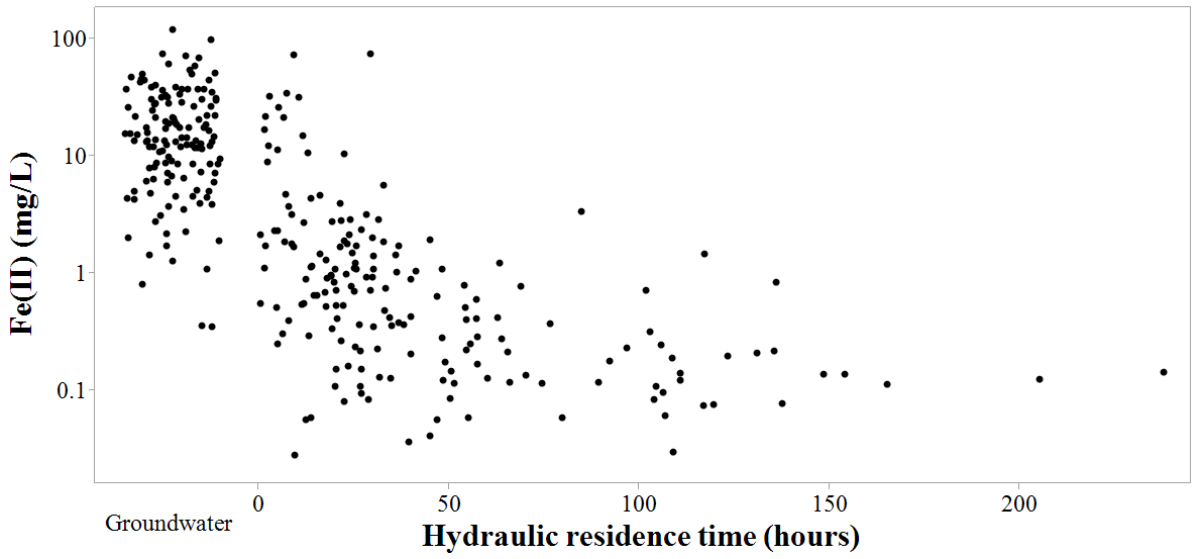

Figure S 13: The dissolved (< 0.45 µm) Fe(II) concentrations in streams (log scale) decrease with increasing hydrological stream order (A) and hydraulic residence time (B). The dissolved Fe(II) concentrations in groundwater are shown on the left of each plot for comparison.

8. The flow and meteorological conditions during sampling

Figure S 15 summarizes the flow and meteorological conditions during the year of this study (2013). Rainfall data were integrated to reflect the rainfall across the Kleine Nete catchment. The average baseflow and interflow contributions to total stream flow during the sampling moments was calculated from the hydrograph measured near the outlet of the Kleine Nete using WETSPRO[12] (Table S 6). A recession constant of 750 h for the baseflow and 80 h for the interflow were used. The Kleine Nete catchment was mostly sampled during dry spells, and the baseflow contribution was large (>80%). Dilution of baseflow by fast components, such as direct interception of rainwater or overland runoff was therefore very limited.

For the studied part of the Demer catchment, no discharge measurements are available, but given its proximity, similar daily rainfall, and similar hydrogeological setting, the flow conditions in both study areas were likely similar. The tributaries to the Demer were sampled during periods of rainfall of low to moderate intensity, except for the November sampling which occurred during a dry spell (Figure S 15). However, the baseflow contribution during each sampling moment was still relatively high (>65%, Table S 6). In order to determine whether this affected streamwater composition and chemistry of the Demer tributaries through dilution of the baseflow by other components, the Ca concentrations and electrical conductivity (EC) in each study area and during each sampling moment are shown (Figure S 14). Even though the Demer tributaries were sampled under variable rainfall conditions, the Ca concentrations and EC exhibit only small variations across the four sampling moments: the median EC in the Demer tributaries ranges between 357 and 449 µS cm^{-1} across the different samplings, and the median Ca concentrations range between 23 and 28 mg L^{-1}. This may be related to the interflow component which partly reflects fast (shallow) groundwater, due to the flat topography and the shallow phreatic groundwater tables (in the valleys usually less than 2 m below the soil surface). In summary, some dilution of groundwater flow by other, more dilute components (such as overland flow or direct interception) may have occurred when the Demer tributaries were sampled. However, the dilution of the groundwater contribution is likely limited, given the relatively large baseflow contribution even during rain events (>65%) and the constant concentrations of conservative solutes (Ca, EC) in streamwater across all samplings. The meteorological conditions did affect the rate of Fe oxidation, but this is discussed in section 9.

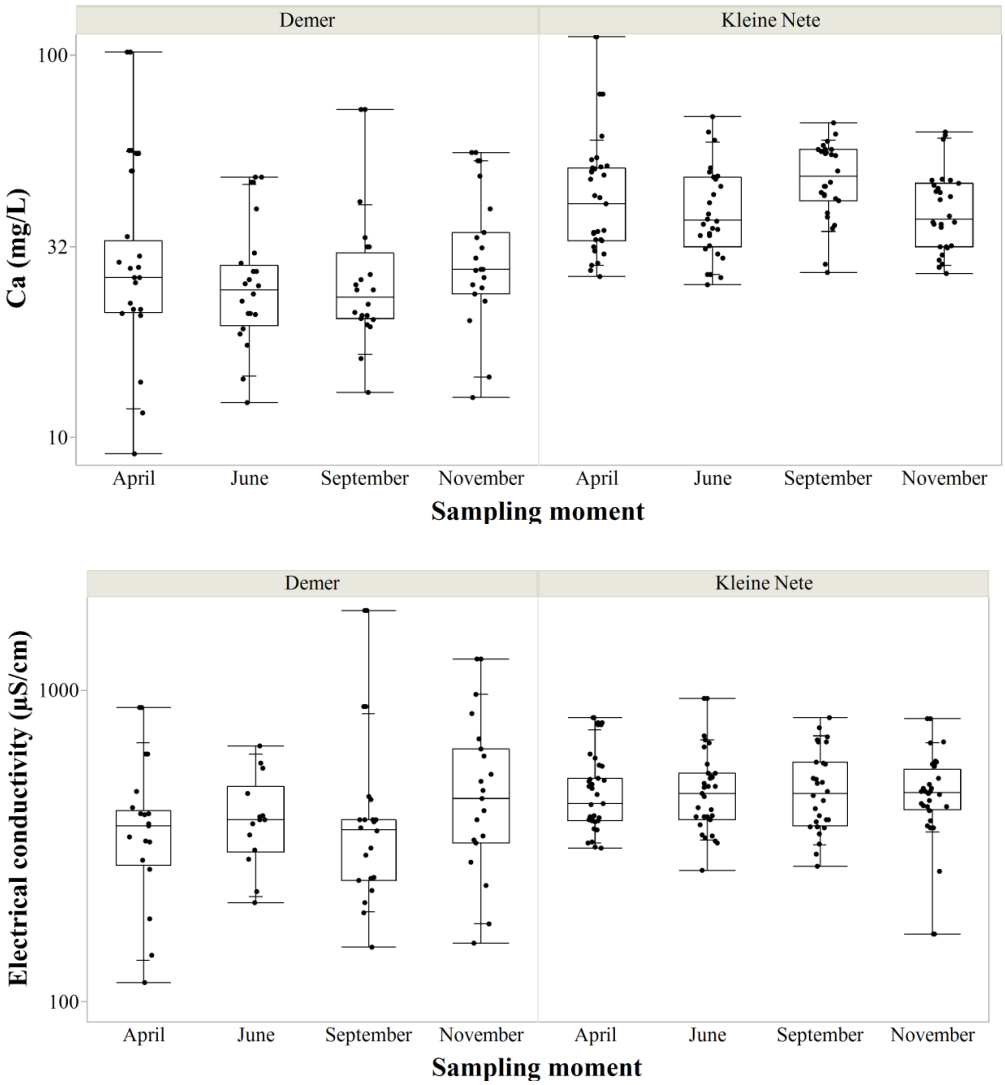

Figure S 14: Calcium concentrations and electrical conductivity in streams of the Demer tributaries and Kleine Nete catchment across the different sampling moments.

Table S 6: Baseflow and interflow contributions to stream flow (in %) during sampling in each study area.

	Kleine Nete		**Demer tributaries**	
	baseflow	*baseflow + interflow*	*baseflow*	*baseflow + interflow*
April 2013	81	92	65	85
June 2013	90	94	72	86
September 2013	86	91	69	88
November 2013	91	94	89	95

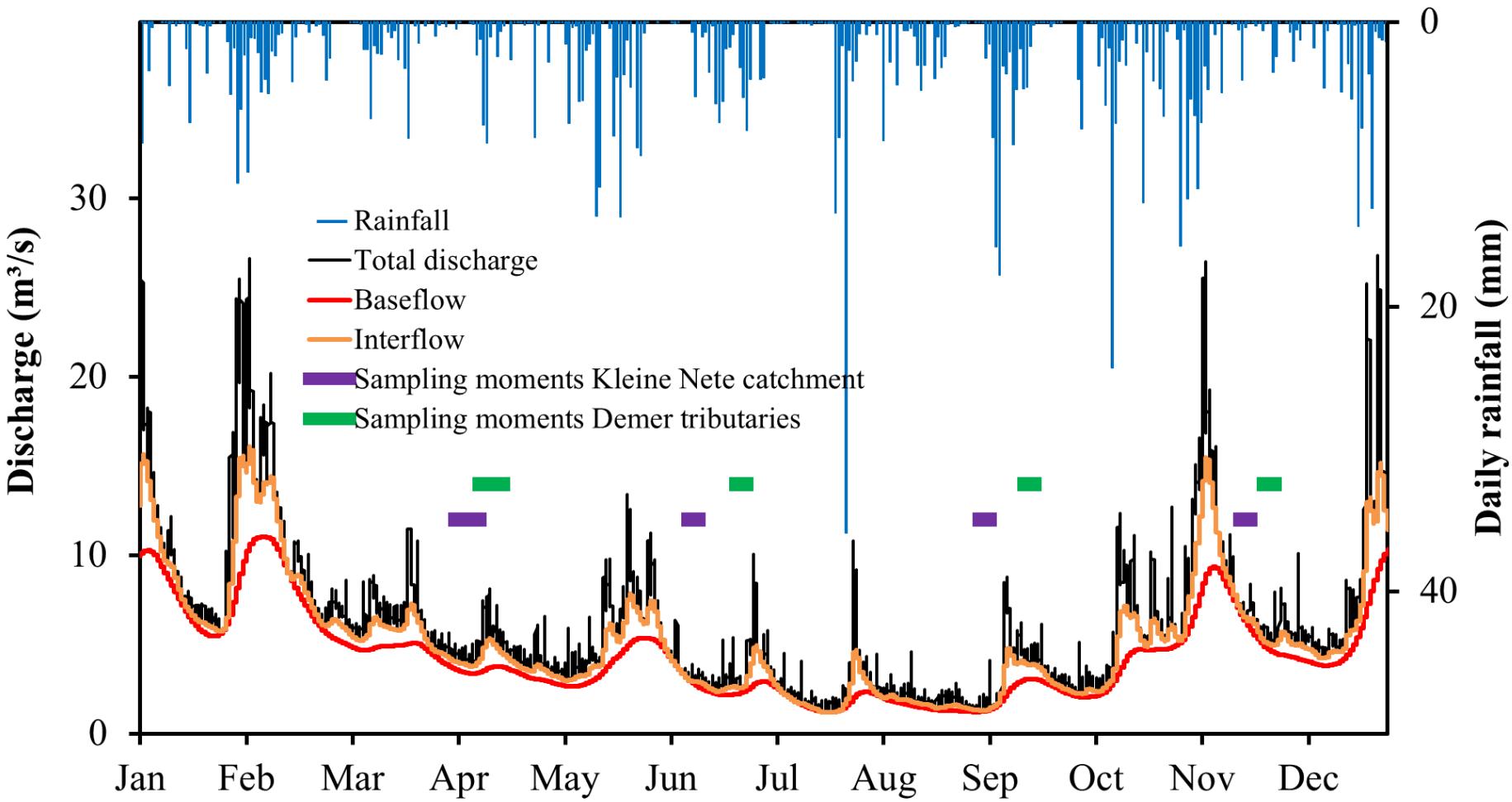

Figure S 15: Total discharge (black) and contributions of baseflow (red) and interflow (orange) during 2013 near the outlet of the Kleine Nete. The baseflow contribution was separated from the total hydrograph using WETSPRO[12]. The integrated daily rainfall across the catchment (blue; secondary vertical axis) and the sampling moments in each study area (purple and green) are indicated.

9. Seasonal effects on the kinetics of Fe(II) oxidation

Table S 7 shows the concentration ranges of total dissolved Fe and of dissolved Fe(II) in streams measured during four samplings throughout the year. Parameters affecting the Fe oxidation reaction (hydrological residence time, O_2 concentration, pH, and temperature) are also presented.

The seasonal variations in Fe concentrations in streams were much less pronounced Demer tributaries compared to the Kleine Nete catchment (Figure S 16). This was likely related to the meteorological conditions at the moment the Demer tributaries were sampled, which were somewhat atypical for the season. The early spring (April) sampling occurred during a remarkably mild period. In contrast, the late summer (September) sampling occurred during a wet and cold period with high flow velocities. This contrasts with the typical average flow velocities, which are higher in winter than in summer. The above atypical conditions caused surprisingly little seasonal variation in water temperature and residence time at the moments the Demer tributaries were sampled. The water temperature ranged only 9—15°C (10^{th}—90^{th} percentile), compared to 7—18°C in the Kleine Nete catchment. The hydrological residence time ranged only 7—58 hours, compared to 8—118 hours in the Kleine Nete catchment. For this reason, the discussion on the seasonality of Fe oxidation kinetics (see main manuscript) is focused on the Kleine Nete catchment.

Table S 8 shows predictions of the mean rate of Fe(II) oxidation in the Kleine Nete near its outlet (at the Grobbendonk permanent monitoring station). Predictions were made for each month of the year using monthly means of pH, O_2 concentration, and stream temperature. Calculations were based on Equation 2 in the main manuscript and on the relationship between temperature and water dissociation[13].

In order to relate the predicted seasonal variability of the Fe oxidation rate (using Equation 2 in the main manuscript) to our measurements of the Fe oxidation gradient in streams, we derived first-order rate constant for the oxidation of Fe(II) based on data of dissolved Fe concentrations in the streams of the Kleine Nete catchment. Plots of the Fe concentrations in streams versus residence time (Figure S 17) show that in two out of four samplings (June and September), only one data point above 3 mg Fe L^{-1} was available, and therefore we were unable to derive oxidation rates for these samplings. During summer, nearly all Fe was already oxidized and removed from the dissolved fraction before it reached the headwaters, likely in the hyporheic zone or in drainage systems. The first-order rate constants were

estimated at $0.06 \pm 0.02\ h^{-1}$ for the April sampling, and at $0.06 \pm 0.01\ h^{-1}$ for the November sampling (error estimates are standard errors). The fitted initial Fe concentrations were 12 ± 3 and $7 \pm 1\ mg\ L^{-1}$, respectively.

		Both study areas				**Demer tributaries**				**Kleine Nete catchment**			
		Apr	**Jun**	**Sept**	**Nov**	**Apr**	**Jun**	**Sep**	**Nov**	**Apr**	**Jun**	**Sep**	**Nov**
Fe	**mean**	5.0	3.2	1.7	4.4	7.4	6.0	3.6	7.3	3.4	1.3	0.3	2.4
	P_{10}	0.5	0.2	0.1	0.5	0.4	0.2	0.2	0.5	0.5	0.2	0.1	0.8
	median	1.5	0.9	0.3	1.7	1.4	1.6	1.0	2.3	1.6	0.7	0.2	1.5
	P_{90}	15.9	3.3	1.6	10.3	30.1	23.0	16.7	33.5	11.1	2.5	0.9	4.5
Fe(II)	**mean**	4.6	2.9	1.5	2.5	7.1	5.8	3.1	3.6	2.9	0.8	0.2	1.8
	P_{10}	0.1	0.1	0.05	0.2	0.03	0.1	0.04	0.1	0.2	0.1	0.1	0.5
	median	0.9	0.3	0.2	1.1	0.6	0.7	0.4	0.6	0.9	0.2	0.1	1.1
	P_{90}	14.7	2.9	1.5	4.5	32.4	23.9	19.7	17.2	11.8	1.3	0.9	4.1
pH	**mean**	6.7	6.6	6.5	6.4	6.6	6.3	6.4	6.6	6.8	6.7	6.6	6.4
	P_{10}	6.3	6.2	6.1	5.6	6.2	5.9	6.0	5.7	6.3	6.3	6.2	5.3
	median	6.7	6.6	6.5	6.6	6.5	6.4	6.3	6.7	6.8	6.7	6.7	6.4
	P_{90}	7.2	7.0	7.1	7.0	7.1	6.6	6.8	7.0	7.3	7.1	7.3	7.0
O_2	**mean**	8.2	6.7	6.2	6.5	6.0	6.3	5.5	6.7	9.4	7.0	6.8	6.4
	P_{10}	5.1	4.7	4.2	4.8	3.9	3.5	3.5	3.2	5.9	4.8	4.2	4.8
	median	7.9	6.8	6.4	6.8	6.3	6.4	5.7	7.0	9.7	7.1	7.1	6.7
	P_{90}	11.1	8.4	8.7	7.9	7.6	7.5	6.9	8.5	11.9	9.4	8.8	7.6
res. time	**mean**	22	50	70	23	16	52	19	28	26	49	106	20
	P_{10}	6	11	9	4	3	10	4	6	5	10	21	4
	median	24	51	39	21	15	46	17	25	27	51	111	20
	P_{90}	35	89	144	45	32	103	37	54	40	75	163	30
temp	**mean**	9	16	16	7	12	14	14	7	7	17	18	8
	P_{10}	5	14	13	6	9	12	12	6	4	14	16	6
	median	8	16	16	8	13	14	13	7	7	17	18	8
	P_{90}	14	18	20	9	15	16	16	9	9	19	21	8

res.time: residence time of the streamwater; watertemp: streamwater temperature; P_{10}: 10^{th} percentile; P_{90}: 90^{th} percentile

Table S 7: The concentrations of total dissolved Fe, dissolved Fe(II) and the factors that affect the kinetics of Fe(II) oxidation in streams, measured on four occasions throughout the year. Data are shown for both study areas (left) and for each study area separately (middle and right).

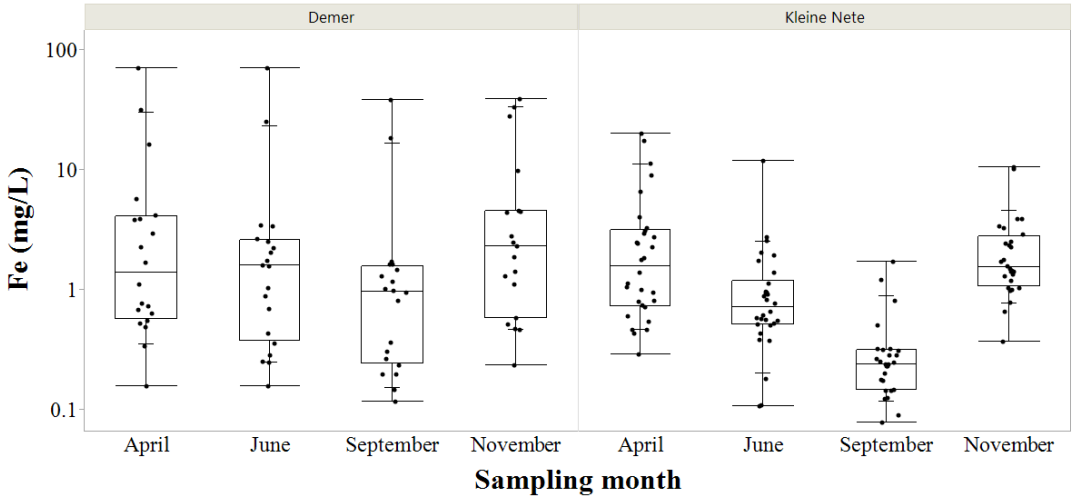

Figure S 16: The total dissolved Fe concentrations in streams (log scale) sampled on four occasions throughout the year. Data are shown for each study area separately.

Table S 8: The abiotic Fe(II) oxidation rate at the outlet of the Kleine Nete catchment in each month of the year, predicted according to Equation 2 in the main manuscript.

	discharge	**T**	**O_2**	**pH**	**oxidation rate**	**half-life**
	m^3 s^{-1}	***°C***	***mg L^{-1}***		***h^{-1}***	***h***
January	11.0	8	11	7.0	0.2	2.8
February	9.0	5	11	6.9	0.1	6.5
March	5.5	8	11	7.1	0.5	1.5
April	4.2	12	10	7.3	1.7	0.4
May	4.5	15	9	7.2	2.0	0.3
June	3.9	17	8	7.4	5.9	0.1
July	4.0	20	8	7.3	6.2	0.1
August	3.2	19	8	7.3	4.7	0.1
September	3.2	16	9	7.3	3.0	0.2
October	4.6	12	9	7.1	0.7	1.0
November	5.6	8	10	7.2	0.5	1.3
December	12.0	6	11	7.0	0.2	4.1

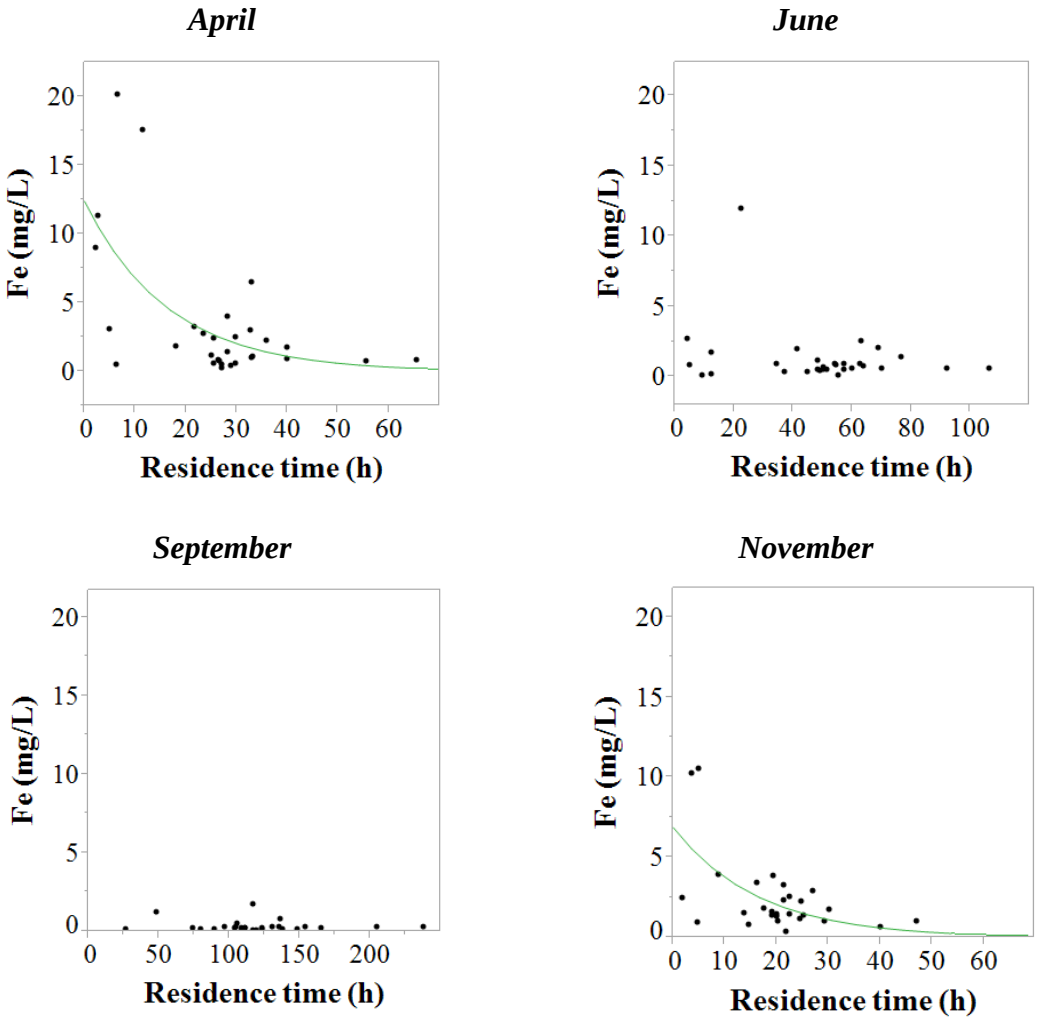

Figure S 17: The dissolved Fe concentrations in streams of the Kleine Nete, plotted against the residence time. The full line is a least-squares fit of an exponential decay curve reflecting Fe(II) oxidation kinetics. In June and September, measured Fe concentrations were low, and no reliable fit could be made.

10. The concentrations of Fe, As, and P in suspended sediment

The concentrations of Fe, P, and As in the suspended sediment of the studied catchments (Table S 9) exceed the typical concentrations of these elements in the soils of the region by up to one order of magnitude. Similar concentrations of Fe and P in suspended sediment were reported in a previous study in the same area[14]. This supports the view that Fe, P, and As are removed from solution by formation of precipitates.

Table S 9: *Aqua regia* extractable concentrations of Fe, P, and As in suspended sediment from the studied catchments (Fe: $n = 57$; P and As: $n = 27$). The typical concentration range of these elements in soils of the region is shown for comparison (data from refs. [15–17]).

	Fe	**P**	**As**
	%	*g kg^{-1}*	*mg kg^{-1}*
minimum	5.1	1.4	13
P_{10}	8.2	2.1	26
median	22.9	7.2	84
P_{90}	38.6	10.2	194
maximum	45.3	10.8	203
typical concentration range in soils	0.3—4	0.4—2	3—15

11. References

(1) Vanlierde, E.; De Schutter, J.; Jacobs, P.; Mostaert, F. Estimating and modeling the annual contribution of authigenic sediment to the total suspended sediment load in the Kleine Nete Basin, Belgium. *Sediment. Geol.* **2007**, *202*, 317–332.

(2) Dekov, V. M.; Vanlierde, E.; Billström, K.; Garbe-Schönberg, C.-D.; Weiss, D. J.; Gatto Rotondo, G.; Van Meel, K.; Kuzmann, E.; Fortin, D.; Darchuk, L.; et al. Ferrihydrite precipitation in groundwater-fed river systems (Nete and Demer river basins, Belgium): Insights from a combined Fe-Zn-Sr-Nd-Pb-isotope study. *Chem. Geol.* **2014**, *386*, 1–15.

(3) Batelaan, O. Phreatology - Characterizing groundwater recharge and discharge using remote sensing, GIS, ecology, hydrochemistry and groundwater modelling, PhD thesis, Vrije Universiteit Brussel, 2006, pp. 1–332.

(4) Batelaan, O.; De Smedt, F. WetSpass: a flexible, GIS based, distributed recharge methodology for regional groundwater modelling. In *Impact of human activity on groundwater dynamics*; Gehrels, H.; Peter, S. N.; Hoehn, E.; Jensen, K.; Leidundgut, C.; Griffioen, J.; Webb, B.; Zaadnoordijk, W. J., Eds.; International Association of Hydrological Sciences: Wallingford, U.K., 2001; pp. 11–17.

(5) Meyus, Y.; Severyns, J.; Batelaan, O.; De Smedt, F. *Ontwikkeling van regionale modellen ten behoeve van het Vlaams Grondwater Model in GMS/MODFLOW. Perceel 1: Het Centraal Kempisch model. Deelrapport 1: Basisgegevens en conceptueel model*; Report to the Flemish Government, Department of Environment and Infrastructure, 2004; pp. 1–126.

(6) Batelaan, O.; De Smedt, F. SEEPAGE, a new MODFLOW DRAIN package. *Ground Water* **2004**, *42*, 576–588.

(7) Viollier, E.; Inglett, P. W.; Hunter, K.; Roychoudhury, A. N.; Van Cappellen, P. The ferrozine method revisited: Fe(II)/Fe(III) determination in natural waters. *Appl. Geochemistry* **2000**, *15*, 785–790.

(8) Jochems, H.; Schneiders, A.; Denys, L.; Van den Bergh, E. *Typologie van de oppervlaktewateren in Vlaanderen*; Report to the Flemish Environment Agency VMM, 2002; pp. 1–67.

(9) AGIV - Agentschap voor Geografische Informatie Vlaanderen. *Vlaamse Hydrografische Atlas*; accessible at http://www.geopunt.be; Ghent, Belgium, 2014.

(10) Vanlierde, E. Sediment concentrations, fluxes and source apportionment: methodology assessment and application in Nete and Demer, PhD thesis, Flanders Hydraulics Research, Antwerp, Belgium, 2013, pp. 1–328.

(11) Matthijs, J.; Lanckacker, T.; De Koninck, R.; Deckers, J.; Lagrou, D.; Broothaers, M. *Geologisch 3D lagenmodel van Vlaanderen en het Brussels Hoofdstedelijk Gewest – versie 2, G3Dv2*; Report to the Flemish Government, Department of Environment, Nature, and Energy, 2013; pp. 1–21.

(12) Willems, P. A time series tool to support the multi-criteria performance evaluation of rainfall-runoff models. *Environ. Model. Softw.* **2009**, *24*, 311–321.

(13) Millero, F. J. Thermodynamics of the carbon dioxide system in the oceans. *Geochim. Cosmochim. Acta* **1995**, *59*, 661–677.

(14) Baken, S.; Sjöstedt, C.; Gustafsson, J. P.; Seuntjens, P.; Desmet, N.; De Schutter, J.; Smolders, E. Characterisation of hydrous ferric oxides derived from iron-rich groundwaters and their contribution to the suspended sediment of streams. *Appl. Geochemistry* **2013**, *39*, 59–68.

(15) *Geochemical Atlas of Europe. Part 1: Background Information, Methodology and Maps*; Salminen, R., Ed.; Geological Survey of Finland: Espoo, Finland, 2005; pp. 1–525.

(16) Tarvainen, T.; Albanese, S.; Birke, M.; Poňavič, M.; Reimann, C. Arsenic in agricultural and grazing land soils of Europe. *Appl. Geochemistry* **2013**, *28*, 2–10.

(17) *Chemistry of Europe's Agricultural Soils, Part A*; Reimann, C.; Birke, M.; Demetriades, A.; Filzmoser, P.; O'Connor, P., Eds.; Schweizerbart Science Publishers: Stuttgart, Germany, 2014; pp. 1–523.